NASA Technical Memorandum 4219

In-Flight Investigation of Shuttle Tile Pressure Orifice Installations

Timothy R. Moes and Robert R. Meyer, Jr.

SEPTEMBER 1990

NASA

NASA Technical Memorandum 4219

In-Flight Investigation of Shuttle Tile Pressure Orifice Installations

Timothy R. Moes and Robert R. Meyer, Jr.
Ames Research Center
Dryden Flight Research Facility
Edwards, California

National Aeronautics and
Space Administration
Office of Management
Scientific and Technical
Information Division

1990

CONTENTS

ABSTRACT

To determine shuttle orbiter wing loads during ascent, wing load instrumentation was added to Columbia (0V-102). This instrumentation included strain gages and pressure orifices on the wing. The loads derived from wing pressure measurements taken during STS 61-C did not agree with those derived from strain gage measurements or with the loads predicted from the aerodynamic database. Anomalies in the surface immediately surrounding the pressure orifices in the thermal protection system (TPS) tiles were one possible cause of errors in the loads derived from wing pressure measurements. These surface anomalies were caused by a ceramic filler material which was installed around the pressure tubing. The filler material allowed slight movement of the TPS tile and pressure tube as the airframe flexed and bent under aerodynamic loads during ascent and descent. Postflight inspection revealed that this filler material had protruded from or receeded beneath the surface, causing the orifice to lose its flushness. Flight tests were conducted at the National Aeronautics and Space Administration (NASA) Ames Research Center Dryden Flight Research Facility to determine the effects of any anomaly in surface flushness of the orifice installation on the measured pressures at Mach numbers between 0.6 and 1.4. An F-104 aircraft with a flight test fixture mounted beneath the fuselage was used for these flights. Surface flushness anomalies typical of those on the orbiter after flight STS 61-C were tested. Also, cases with excessive protrusion and recession of the filler material were tested.

This report shows that the anomalies in STS 61-C orifice installations adversely affected the pressure measurements. But the magnitude of the affect was not great enough to account for the discrepancies with the strain gage measurements and the aerodynamic predictions.

NOMENCLATURE

BLF	boundary-layer fence
BLTD	boundary-layer thickening device
C_p	pressure coefficient, $(p - p_\infty)/\bar{q}$
Cp_{ref}	pressure coefficient at the center reference orifice
Cp_{test}	pressure coefficient at the test orifice
FRCI	fibrous refractory composit insulation
FTF	flight test fixture
h_p	pressure altitude, ft
HRSI	high-temperature reusable surface insulation
M_∞	free-stream Mach number
OV-102	Orbiter Columbia (used for STS 61-C)
p_∞	free-stream static pressure, lb/ft^2
$\bar{q}$	incompressible dynamic pressure, lb/ft^2
Rn/ft	unit Reynolds number/ft
SIP	strain isolation pad
STS 61-C	shuttle transportation system flight 61-C
TPS	thermal protection system
x/c	ratio of distance from the leading edge to total length of the FTF
α	angle of attack, deg
ΔCp	pressure coefficient error, $Cp_{test} - Cp_{ref}$

INTRODUCTION

To verify predictions of wing load during ascent, the shuttle orbiter Columbia (OV-102) was instrumented with multiple strain gages and pressure orifices on the wing. Initial wing pressure measurements were obtained during the orbiter flight test program (STS 1–5). There were not enough orifices, however, to adequately determine the wing pressure distributions for an accurate determination of wing loads. Consequently, additional orifices were added to OV-102. The STS 61-C mission in January 1986 was the first shuttle flight to obtain extensive wing pressure measurements. The unpublished loads data from flight 61-C wing pressure measurements did not agree with the loads predicted from the aerodynamic database or with the loads determined from strain gage measurements (fig. 1). Also, the pressures measured during flight 61-C did not agree with those measured in the earlier STS 1–5 flights. The installation technique of the pressure orifices in the thermal protection system (TPS) tiles was believed to be one cause of the discrepancy. The installation technique used for STS 61-C was different from that for STS 1–5.

Because of the brittleness of the TPS tiles, a ceramic cloth gap filler was used to separate the tile from the stainless steel pressure tube for STS 61-C. The gap filler allowed relative movement between the tile and pressure orifice tube during wing flexing and prevented the pressure tube from damaging the tile. Inspection of the orifices after flight 61-C showed that the gap filler did not always remain flush with the tile surface. Gracey (1980) and Livesey, Jackson, and Southern (1962) show that if the surface near the orifice is not flush, it can lead to significant errors in local pressure measurements. Although the anomalies in the shuttle pressure orifice installations led to measurement errors, there was no way to estimate confidently the magnitude of these errors. Therefore, a flight test program was conducted at the NASA Ames Research Center Dryden Flight Research Facility to quantitatively determine the affects of the orifice anomalies on the measured pressures.

Figure 2 shows a typical TPS tile orifice after STS 61-C. The gap filler material was usually recessed into the hole surrounding the pressure tube, although in some cases it protruded from it. The deformation of the orifice installations was attributed to reentry heating, improper installation, or air loads. For this experiment, test panels contained recessed, protruding, and nearly flush gap filler installations. These panels were flight-tested on an F-104 aircraft with a flight test fixture (FTF) mounted on its undersurface. Stabilized test points were flown at dynamic pressures similar to shuttle launch conditions for Mach numbers between 0.6 and 1.4. This report describes the flight test techniques used to analyze the orifice installations. It also describes the orifice installations and presents the results from the flight tests.

DESCRIPTION OF TEST FACILITY

The F-104 Aircraft

A specially equipped F-104 aircraft was used as a carrier vehicle for these experiments because it is capable of obtaining the shuttle Mach number and dynamic pressure profile of interest. It was modified to carry a lower fuselage fin, the FTF, on which the test articles were installed. An airdata probe mounted on the noseboom was used to obtain free-stream airdata parameters such as Mach, altitude, and dynamic pressure. Figure 3 shows the F-104 airplane with the FTF. The aircraft was also instrumented with special cockpit displays (Meyer and Schneider, 1983) that allowed for precise Mach and dynamic pressure flight profiles, which generally matched orbiter launch conditions.

Flight Test Fixture, Test Panel, and Instrumentation

A detailed description of the FTF and its capabilities is presented by Meyer (1981). The FTF had a chord of 80 in. and extended 24 in. beneath the F-104 fuselage. A rigid foam panel simulating the orbiter wing surface, was attached to the right side of the FTF, as figure 4 shows. The TPS tile test articles were then attached to cavities

within this foam panel to allow for realistic gaps and steps between the test article and the foam panel. The tiles were also oriented to surface streamlines as on the orbiter. Both a forward and an aft position were provided for the test articles (fig. 4). This allowed simultaneous flight test of two identical tiles to determine if the results would be similar at different FTF chord locations. In addition to the test articles, flush pressure orifices were installed along the length of the FTF to obtain a pressure distribution along the chord. For consistency in the flight data, a grit strip at the 5-percent chord location was used to insure boundary-layer transition from laminar to turbulent flow. A boundary-layer rake was used to measure the thickness of the boundary layer aft of the test articles. On some flights a boundary-layer thickening device (BLTD) was located at the 20-percent chord location to increase the thickness of the turbulent boundary layer. The BLTD consisted of forty-five 0.138-in. diameter machine screws on a metal strip that spanned the fin. The screws were spaced every 0.31 in. and the shaft end extended 0.25 in. above the surface. Figure 5 shows the BLTD. Figure 4 also shows the locations of the grit strip and BLTD.

The FTF surface and boundary-layer pressures were measured by a 48-port mechanical differential pressure scanning transducer, two 32-port electronically scanned multiple-differential pressure transducer assemblies, and two absolute pressure transducers. Pressure measurements were estimated to be accurate to within ± 2.5 lb/ft^2 which represents approximately 0.005 Cp at the design launch profile and approximately 0.01 Cp at the low Reynolds number test points.

TEST ARTICLE DETAILS

For this experiment, eight silicon fibrous refractory composite insulation 12 (FRCI 12) tiles were constructed. This is the type of TPS tile used for the high-temperature reusable surface insulation (HRSI) which covers much of the orbiter wing's lower surface and the outboard portions of the wing's upper surface. Figure 6 shows the dimensions of the tiles. Each tile was a square, 6 in. on a side, and contained four orifices. On most tiles, two were test orifices, one a primary reference orifice, and the fourth a secondary reference orifice, which was used as a backup for the primary reference orifice (fig. 6(a)). Two of the tiles contained four reference orifices which verified the uniformity of the pressure distribution across the tile when flown on the FTF. The tiles were bonded to a 0.25-in. aluminum plate for mounting to the FTF. Two of the eight tiles were fabricated with a strain isolation pad (SIP) between the aluminum plate and the tile (fig. 6(b)). The tiles with the SIP installation are more representative of the actual shuttle tile installation than the six remaining tiles which did not contain an SIP (fig. 6(c)).

The reference orifices were 0.08 in. in diameter and flush with the tile surface, as shown in figure 7(a). The test orifices were installed within a 0.5-in. diameter hole in the tile. The aluminum pressure tube had a 0.086 in. inner diameter and 0.125 in. outer diameter. Figures 7(b) through 7(m) show the orifices tested in this experiment. The exposed surface of the gap filler was shaped to simulate orifice region anomalies on the orbiter after flight 61-C. The test orifices varied from nearly flush (test orifices 1 through 4) to excessively distorted (test orifices 5 and 6). The excessively protruding gap filler installations of test orifices 5 and 6 were not typical of those found on the orbiter after flight 61-C but were tested to extend the database.

FLIGHT TEST APPROACH AND MANEUVERS

The basic approach of this experiment was to fly stabilized test points that would simulate Mach numbers and dynamic pressures experienced by the orbiter on a typical launch. As previously stated, the F-104 was suitable for this experiment because it is capable of flying the portion of the orbiter Mach number and dynamic pressure profile which includes the maximum dynamic pressure condition. Table 1 lists the free-stream conditions and the test orifice pressures for each test point. Each test point consisted of approximately 30 seconds of stabilized flight at the specified Mach number and altitude. Figure 8 shows the test conditions flown in this experiment and the design dynamic pressure profile for the orbiter. Points were flown both at or near the design dynamic pressure and at approximately one-third of the design dynamic pressure to lower the Reynolds number for certain test points.

Increasing the obtainable boundary-layer thickness on the FTF was also considered for this experiment. Although it was impossible to generate the large turbulent boundary layers obtained on the orbiter wing, two approaches were used to thicken the FTF boundary layer. The first approach involved flying each design Mach number at a higher altitude, determined by reducing the Reynold's number by half. A thicker boundary layer would then be obtained since boundary-layer thickness increases as Reynolds number decreases. However, with this method the dynamic pressure was less for each Mach number. The second method of increasing the boundary-layer thickness used the BLTD at the 20-percent chord location of the FTF.

TEST RESULTS AND DISCUSSION

Flight Test Fixture Pressure Distributions

The two tile test sections were located in a region where the pressure distribution on the FTF chord was relatively flat for the range of Mach numbers studied. This would give similar local velocities and pressures at the two test sections even though the boundary layer would be slightly thicker for the aft test section. Figure 9 shows a series of typical pressure distributions along the chord. The forward test section is located at x/c = 0.584 and the aft test section is located at x/c = 0.794. For the cases below Mach 1.3, the local pressure is slightly more positive (lower local velocities) at the forward test section than at the aft test section. At Mach 1.30, the local conditions are approximately the same for both test sections. At Mach 1.39, the local pressure at the forward test section is considerably lower than the local pressure at the aft test section.

Boundary-Layer Measurements

As previously mentioned, two approaches were used to increase the thickness of the FTF boundary layer. Typical results from these two methods can be seen in the measured boundary-layer thicknesses shown in figure 10. By decreasing the Reynolds number, a small increase in boundary-layer thickness can be observed for subsonic cases. In the transonic region, data trends are confusing, probably because of the interaction of shock and boundary layer. The BLTD method was more successful in increasing the boundary-layer thickness than flying at lower Reynolds numbers. The installation of the BLTD increased the boundary-layer thickness by approximately 30 percent for the subsonic and supersonic cases.

Reference Orifices

The two initial flights of the program were used to document the distribution of test-panel surface static pressures. Comparing pressures measured at the different reference orifices distributed vertically on the tile showed that there were no major vertical pressure gradients. Figure 11 shows the difference in pressure coefficient (ΔCp) between coefficients of pressure of the reference orifices at the test locations (Cp_{test}) and those at the center reference orifices (Cp_{ref}). With the exception of the data for reference orifice R1 (circular symbols), the pressure coefficient differences were less than 0.01. A chip at the edge of reference orifice R1 may have adversely affected the pressure measurement at that location. The other three orifice test locations consistently measured slightly higher pressure than the center orifices indicating slight vertical pressure gradients. However, these gradients were not large enough to mask the affects of the test orifice installations. The data for the test configurations will not be corrected for these small pressure gradients.

Test Orifices

The basic results for test orifices 1 through 12 are shown in figures 12 through 17. The ΔCp is plotted for each test orifice, and the data are separated according to whether or not the boundary-layer fence was installed while obtaining data.

Affect of the Boundary-Layer Thickening Device on Test Orifice Pressure Error

Figure 18 shows the affect of the BLTD on ΔCp values for test orifices 1, 8, and 12. The thickened boundary layer had a small affect on the local differential pressure coefficients. The affect was largest for the supersonic test points, which in most cases showed a decrease in ΔCp values (less negative) with the increased boundary-layer thickness. The results from the other orifices (figs. 12 to 17) show similar affects of increased boundary-layer thickness.

Affect of Reynolds Number on Test Orifice Error

Reynolds number had a small, but noticeable, affect on the ΔCp values for the test orifices. As can be seen in figures 12 to 17, the test orifice errors for the low Reynolds number cases ($\approx 2 \times 10^6$/ft) were consistently lower than errors for cases flown at higher Reynolds numbers ($\approx 4 \times 10^6$/ft). This was expected since the critical roughness height is lower for high unit Reynolds numbers (Schlicting, 1979).

Test Orifices 1, 2, 3, and 4

Test orifices 1, 2, 3, and 4 had nearly flush gap filler and showed similar results. Orifices 1 and 2 were installed on tiles with SIP. Because of the similarity of the results between orifices mounted on SIP and those not mounted on SIP, it was determined that the SIP had no affect on the results. The magnitude of the test orifice errors was less than 0.03 Cp for the orifices in the forward test section. An error of between -0.01 Cp and -0.04 Cp was observed for the orifices in the aft test section. These results can be seen in figures 12 and 13.

The aft test locations consistently showed a ΔCp 0.02 more negative than the forward test locations. The lowest (most extreme) ΔCp values tended to occur near Mach 0.9. The differences in local pressure at the test sections, as well as slight differences in the orifice installations, are believed to cause the discrepancy between the forward and aft test locations. The scatter in the data for each orifice is mostly attributed to the affects of Reynolds number.

Test Orifices 5 and 6

Test orifices 5 and 6 both had an excessive amount of gap filler protruding above the tile surface. The ΔCp values for their test orifices are plotted in figure 14. The maximum magnitude of the ΔCp values was approximately -0.12 for the forward location (orifice 5) and -0.17 for the aft location (orifice 6). The differences between the forward and aft test locations increased with Mach number, from 0.04 ΔCp at the low Mach numbers to 0.09 ΔCp at the high Mach numbers.

Test Orifices 7 and 8

Figure 15 shows data for test orifices 7 and 8. On these orifices, the gap filler protruded slightly above the tile surface. The height of the gap filler above the tile surface was less than that for orifices 5 and 6, therefore the magnitudes of the ΔCp values were also less. The most extreme ΔCp values were about -0.08. The aft location (orifice 8) had ΔCp values of 0.02 to 0.04 more negative than the forward location (orifice 7).

Test Orifices 9 and 10

Data for test orifices 9 and 10 are shown in figure 16. These orifices contained gap filler recessed beneath the tile surface and around the pressure tubing. The most extreme ΔCp values were about -0.05. Unlike the previous orifices, the aft location (orifice 10) showed a less extreme ΔCp value than the forward location (orifice 9). The influence of Mach number on ΔCp for these orifice anomalies was significantly less than for the protruding gap filler anomalies.

Test Orifices 11 and 12

Test orifices 11 and 12 contained gap filler recessed beneath the surface but also had a slight amount of gap filler protruding at the edges of the orifice. The results are shown in figure 17 with ΔCps between -0.04 and -0.09 at the low Mach numbers and between -0.01 and -0.05 at the higher Mach numbers. These ΔCp values were considerably larger than those for the orifices with only recessed gap filler. The slight protrusion of gap filler, therefore, plays a significant role in adversely affecting the pressure measurement. As with the recessed gap filler orifices (9 and 10), the aft location (orifice 12) showed a smaller value of ΔCp then the forward location (orifice 11). The difference in ΔCp between the forward and aft locations was approximately 0.03.

General Trends

Figures 12 through 17 show that ΔCp is fairly constant for Mach numbers between approximately 0.7 and 1.2. As Mach number increased beyond 1.2, the affects of the orifice anomalies generally became less. Some ΔCp values for gap filler anomalies could be approximately characterized by the amount of recession or protrusion of gap filler. These ΔCp values are compiled in figure 19 and represent the average error for Mach numbers between 0.7 and 1.2. For the protruding gap filler cases, the error associated with the amount of protrusion seemed well defined. The approximate amount of error caused by the recessed gap filler showed no well defined trend. The ΔCps are negative, in agreement with results from Gracey (1980). The flushness of the orifice is critical to accurate pressure measurements, and protruding gap filler is a more serious problem than recessed filler.

CONCLUSIONS

The objective of this study was to quantify the affects of the OV-102 pressure orifice irregularities on the pressures measured during flight STS 61-C. This included testing nearly flush orifice installations as well as anomalies typical of those observed after STS 61-C. The F-104 FTF was used because of its large Mach number and dynamic pressure envelope, allowing the test articles to be exposed to realistic airloads.

For the nominal shuttle orifice (those without excessively protruding gap filler), there were noticeable pressure measurement errors caused by the gap filler installation. These were typically less than 0.05 in Cp and therefore did not account for the entire discrepancy in the flight data that motivated this experiment. The amount of error in the pressure measurement was basically proportional to the physical dimensions of the anomaly. The protrusion of the gap filler material caused greater errors in pressure measurement than recessed gap filler.

REFERENCES

Gracey, William, *Measurement of Aircraft Speed and Altitude*, NASA RP-1046, 1980.

Livesey, J.L., J.D. Jackson, and C.J. Southern, "The Static Hole Error Problem. An Experimental Investigation of Errors for Holes of Varying Diameters and Depths," Aircraft Engineering, Feb. 1962.

Meyer, Robert R., Jr., *A Unique Flight Test Facility: Description and Results*, NASA TM-84900, 1982.

Meyer, R.R., Jr., and Cd. E.T. Schneider, "Real-Time Pilot Guidance System for Improved Flight Test Maneuvers," AIAA-83-2747, 1983.

Schlicting, Hermann, *Boundary-Layer Theory*, 7th ed., McGraw-Hill Book Co., 1979.

Table 1. Flight conditions and orifice pressures for each test point.

(a) Data for reference orifices R1, R2, R3, and R4 without the BLTD installed.

Flight conditions						Local pressures (lb/ft^2)					
					Rn/ft	Forward			Aft		
M_∞	h_p	P_∞	$\bar{q}$	α	$\times 10^6$	reference	R1	R2	reference	R3	R4
0.598	7,848.	1,581.1	395.5	4.97	3.2	1,570.2	1,575.8	1,572.2	1,562.4	1,563.0	1,564.6
0.794	33,628	531.4	234.6	7.15	2.0	535.7	539.3	538.1	527.3	528.6	529.9
0.795	12,214	1,334.6	590.8	3.55	3.8	1,301.3	1,311.0	1,302.0	1,283.7	1,284.5	1,288.1
0.797	12,190	1,335.9	593.2	3.48	3.8	1,302.0	1,311.5	1,304.7	1,285.5	1,286.0	1,288.9
0.849	13,705	1,257.9	634.4	3.35	3.9	1,221.3	1,230.4	1,224.2	1,196.6	1,197.0	1,200.6
0.889	36,033	474.0	262.3	6.31	2.0	475.2	480.2	477.6	461.0	461.7	464.6
0.890	15,152	1,187.0	658.4	3.06	3.9	1,147.9	1,158.5	1,149.4	1,114.0	1,114.3	1,119.5
0.891	35,968	475.5	264.5	6.78	2.1	478.7	483.2	480.6	465.0	464.8	467.0
0.901	8,010	1,571.3	893.6	2.45	4.8	1,507.2	1,524.1	1,509.4	1,460.3	1,460.1	1,465.9
0.902	15,195	1,184.9	674.5	2.99	3.9	1,142.2	1,153.6	1,143.3	1,107.6	1,108.3	1,112.6
0.902	8,054	1,568.6	893.8	2.47	4.8	1,505.5	1,519.9	1,507.5	1,458.0	1,456.3	1,462.9
0.949	16,980	1,102.0	694.9	3.00	3.9	1,080.3	1,091.0	1,079.6	1,042.1	1,041.8	1,046.7
1.050	17,989	1,057.3	816.7	2.75	4.2	1,081.9	1,091.4	1,084.7	1,045.7	1,046.7	1,051.9
1.098	22,209	885.8	748.0	3.07	3.9	932.5	941.2	935.5	882.1	882.4	887.4
1.101	40,066	390.5	331.3	5.14	2.2	425.8	428.0	427.7	416.5	416.8	418.8
1.202	25,003	785.2	793.5	2.62	3.9	859.3	865.0	858.6	841.9	840.7	846.9
1.243	42,456	348.1	376.4	5.64	2.2	392.3	396.2	392.0	402.6	402.4	405.1
1.373	46,731	283.4	374.1	5.29	2.0	318.0	322.2	314.9	342.5	341.7	342.8

(b) Data for test orifices 1, 9, 2, and 10 with BLTD installed.

Flight conditions						Local pressures (lb/ft^2)					
					Rn/ft	Forward			Aft		
M_∞	h_p	P_∞	$\bar{q}$	α	$\times 10^6$	reference	1	9	reference	2	10
0.597	7,788	1584.7	395.9	4.93	3.3	1,584.1	1,578.9	1,569.8	1,573.0	1,562.9	1,567.3
0.704	12,198	1,335.4	462.8	4.38	3.4	1,330.6	1,324.8	1,313.6	1,316.1	1,302.6	1,307.5
0.802	33,599	532.1	239.3	6.70	2.0	542.2	538.9	534.0	531.6	524.9	527.2
0.803	12,178	1,336.5	603.8	3.29	3.9	1,321.1	1,313.7	1,298.3	1,297.9	1,279.4	1,287.3

Table 1. Continued

(b) Concluded.

	Flight conditions					Local pressures (lb/ft^2)					
					Rn/ft	Forward			Aft		
M_∞	h_p	P_∞	$\bar{q}$	α	$\times 10^6$	reference	1	9	reference	2	10
0.848	13,685	1,259.0	634.1	3.05	4.0	1,241.9	1,232.7	1,218.9	1,212.8	1,194.3	1,200.4
0.848	33,947	523.4	263.4	6.43	2.1	533.7	531.5	524.8	520.3	512.8	515.8
0.851	13,681	1,259.1	638.1	2.99	3.9	1,243.8	1,232.0	1,216.7	1,212.0	1,193.3	1,200.9
0.898	15,179	1,185.7	668.7	2.77	4.0	1,168.2	1,159.2	1,141.6	1,129.5	1,106.8	1,113.9
0.900	7,939	1,575.6	892.9	2.25	4.9	1,542.5	1,526.1	1,505.7	1,489.4	1,459.8	1,470.1
0.903	33,980	522.6	298.6	5.34	2.2	530.3	528.2	519.4	511.3	502.1	508.1
0.948	16,950	1,103.4	694.0	2.68	4.0	1,103.4	1,093.8	1,074.9	1,061.4	1,039.5	1,046.2
0.948	16,964	1,102.8	693.2	2.72	4.0	1,105.8	1,093.9	1,073.9	1,060.2	1,038.7	1,046.0
1.106	22,154	887.9	760.3	3.04	4.0	971.1	958.3	944.2	912.0	890.2	895.6
1.116	20,037	971.0	846.2	2.73	4.3	1,056.8	1,040.2	1,029.4	996.1	971.8	979.9
1.153	22,254	884.1	822.2	2.59	4.1	968.6	952.3	944.0	927.7	905.3	912.5
1.200	22,025	892.8	900.0	2.33	4.4	990.9	978.8	965.9	970.7	947.2	953.1
1.201	25,032	784.2	791.9	2.55	4.0	876.6	866.3	854.8	858.6	837.1	843.1
1.302	27,024	718.4	852.8	1.70	4.0	807.6	805.2	798.5	817.5	798.2	801.7
1.392	29,825	633.5	859.0	2.26	4.0	592.6	604.9	557.9	757.0	749.9	740.7
1.393	39,841	394.7	536.3	3.34	2.7	396.5	405.0	375.2	487.3	480.7	475.9

(c) Data for test orifices 1, 9, 2, and 10 without BLTD installed.

	Flight conditions					Local pressures (lb/ft^2)					
					Rn/ft	Forward			Aft		
M_∞	h_p	P_∞	$\bar{q}$	α	$\times 10^6$	reference	1	9	reference	2	10
0.801	12,197	1,335.5	600.5	3.29	4.0	1,320.2	1,311.8	1,296.9	1,298.1	1,278.2	1,286.0
0.849	33,990	522.4	263.4	6.34	2.1	530.6	529.0	521.9	518.3	510.3	513.9
0.851	13,700	1,258.2	638.5	3.04	4.0	1,241.6	1,230.5	1,216.8	1,211.6	1,190.8	1,199.1
0.897	33,994	522.3	294.0	5.54	2.2	529.3	528.0	519.3	513.2	503.6	507.1
0.904	15,204	1,184.5	677.8	2.77	4.1	1,167.4	1,155.6	1,138.4	1,124.5	1,100.1	1,108.8
0.947	16,988	1,101.7	692.1	2.58	4.1	1,099.7	1,088.6	1,068.8	1,057.2	1,035.4	1,041.3
1.116	20,028	971.4	846.9	2.57	4.4	1,050.8	1,030.8	1,017.6	993.7	966.8	975.4
1.196	21,946	895.8	897.0	2.39	4.4	996.0	975.9	960.3	973.1	945.1	951.9
1.300	27,010	718.8	850.0	2.09	4.1	824.8	825.9	815.5	823.4	799.9	803.6

Table 1. Continued

(d) Data for test orifices 3, 5, 4, and 6 with BLTD installed.

Flight conditions						Local pressures (lb/ft^2)					
					Rn/ft	Forward			Aft		
M_∞	h_p	P_∞	$\bar{q}$	α	$\times 10^6$	reference	3	5	reference	4	6
0.597	7,837	1,581.7	395.1	4.90	3.3	1,575.4	1,570.6	1,531.7	1,565.5	1,553.8	1,506.3
0.700	7,953	1,574.7	539.5	3.87	3.9	1,557.7	1,550.1	1,498.4	1,543.2	1,525.4	1,461.8
0.702	12,206	1,335.0	461.0	4.36	3.5	1,323.4	1,317.5	1,272.3	1,310.5	1,296.0	1,241.9
0.793	12,169	1,336.9	589.0	3.41	3.9	1,313.5	1,306.8	1,247.4	1,294.8	1,274.3	1,203.8
0.796	7,952	1,574.8	699.2	2.85	4.4	1,541.8	1,532.0	1,463.4	1,517.9	1,495.0	1,412.9
0.796	33,567	532.9	236.6	7.68	2.1	540.6	538.7	518.1	531.0	523.8	495.7
0.845	13,652	1,260.6	630.2	3.21	4.0	1,236.4	1,227.0	1,164.0	1,208.8	1,188.0	1,107.4
0.848	33,949	523.4	263.4	6.69	2.2	528.2	526.4	500.7	516.8	509.7	476.7
0.893	7,962	1,574.2	878.9	2.42	5.0	1,529.4	1,515.3	1,421.9	1,478.7	1,446.7	1,331.0
0.894	33,998	522.2	292.4	5.67	2.3	524.1	521.6	491.4	507.7	497.0	459.5
0.904	24,936	787.5	450.3	3.79	3.0	777.9	771.1	723.1	748.6	733.9	672.4
0.905	15,186	1,185.4	680.2	2.80	4.1	1,157.0	1,148.2	1,075.2	1,113.5	1,089.3	999.7
0.949	17,001	1,101.1	694.2	2.59	4.0	1,087.2	1,076.5	1,005.2	1,044.0	1,020.6	925.7
1.106	20,017	971.8	832.0	2.84	4.3	1,042.1	1,028.0	960.6	980.4	952.7	839.4
1.108	19,969	973.8	837.2	2.64	4.3	1,041.0	1,026.1	955.0	979.9	953.5	838.7
1.185	21,991	894.1	878.7	2.65	4.4	981.4	967.6	906.7	955.4	929.2	819.8
1.200	22,003	893.6	900.2	2.12	4.4	977.0	966.2	907.8	961.2	935.0	822.6
1.293	26,992	719.4	841.5	1.92	4.1	813.5	814.9	788.6	810.4	788.9	708.0
1.299	24,985	785.8	928.0	1.87	4.4	883.8	883.7	859.4	888.6	862.5	777.8
1.390	29,770	635.1	858.5	2.60	4.1	603.6	620.4	530.4	769.6	759.9	694.9
1.394	24,846	790.6	1075.2	1.91	4.7	710.8	721.9	618.5	923.7	911.3	832.4

Table 1. Concluded

(e) Data for test orifices 7, 11, 8, 12 with the BLTD installed.

Flight conditions						Local pressures (lb/ft^2)					
					Rn/ft	Forward			Aft		
M_∞	h_p	P_∞	$\bar{q}$	α	$\times 10^6$	reference	7	11	reference	8	12
0.702	12,206	1,335.0	459.9	4.24	3.4	1,324.7	1,302.7	1,291.3	1,303.1	1,272.6	1,278.8
0.791	33,595	532.2	233.3	6.90	2.0	537.6	529.4	523.4	524.2	510.4	514.1
0.797	12,228	1,333.8	593.2	3.37	3.9	1,313.1	1,285.0	1,267.6	1,278.8	1,238.0	1,249.6
0.802	8,020	1,570.7	707.2	2.93	4.4	1,543.4	1,504.9	1,485.5	1,500.5	1,450.7	1,466.3
0.847	13,721	1,257.1	630.8	2.59	4.0	1,226.7	1,194.7	1,175.1	1,186.0	1,140.8	1,153.3
0.847	33,912	5,24.3	263.2	6.68	2.1	530.3	520.5	513.5	512.3	496.3	500.8
0.898	15,193	1,185.0	669.1	2.81	4.0	1,159.3	1,119.9	1,103.8	1,099.2	1,048.8	1,067.0
0.899	33,977	522.7	296.0	5.96	2.2	527.6	515.5	507.6	502.8	482.8	490.0
0.902	7,987	1,572.7	894.7	2.26	4.9	1,530.6	1,473.3	1,451.6	1,450.6	1,376.9	1,403.0
0.949	16,999	1,101.2	694.5	2.54	4.0	1,091.1	1,048.4	1,035.0	1,025.3	971.3	992.0
1.114	20,031	971.3	844.2	2.91	4.3	1,050.7	1,012.6	996.9	967.1	906.2	931.9
1.199	21,985	894.3	899.3	2.35	4.3	984.3	955.2	937.5	943.7	884.2	911.2
1.304	27,072	716.9	853.2	1.79	4.0	803.8	799.5	789.6	794.8	747.0	772.2
1.397	29,830	633.3	865.7	1.65	4.0	563.9	553.9	518.2	722.4	700.2	704.4

(f) Data for test orifices 7, 11, 8, and 12 without BLTD installed.

Flight conditions						Local pressures (lb/ft^2)					
					Rn/ft	Forward			Aft		
M_∞	h_p	P_∞	$\bar{q}$	α	$\times 10^6$	reference	7	11	reference	8	12
0.846	33,895	524.7	262.8	6.70	2.0	532.4	522.8	516.0	515.5	497.4	504.3
0.897	33,944	523.5	294.9	5.94	2.2	529.4	517.2	509.0	505.2	483.8	492.6
1.107	19,873	977.7	839.4	2.86	4.1	1,051.5	1,000.1	989.5	969.3	897.0	931.4
1.198	21,907	897.3	900.9	2.55	4.2	991.7	946.9	932.2	951.4	881.2	917.1
1.302	26,926	721.6	855.6	2.84	3.9	835.9	831.5	820.7	819.5	759.2	793.1
1.396	29,787	634.6	865.8	2.16	3.9	572.5	566.7	524.9	739.1	704.8	716.7

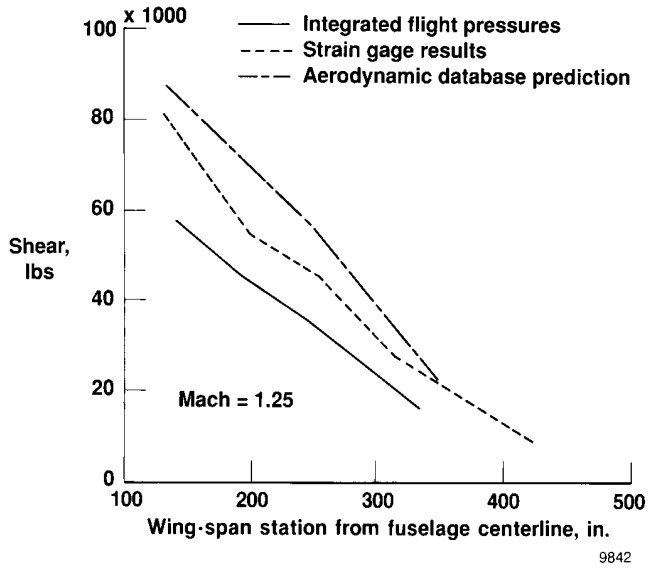

Figure 1. Wing-root shear loads from STS 61-C strain gage, pressure measurements, and the aerodynamic database prediction.

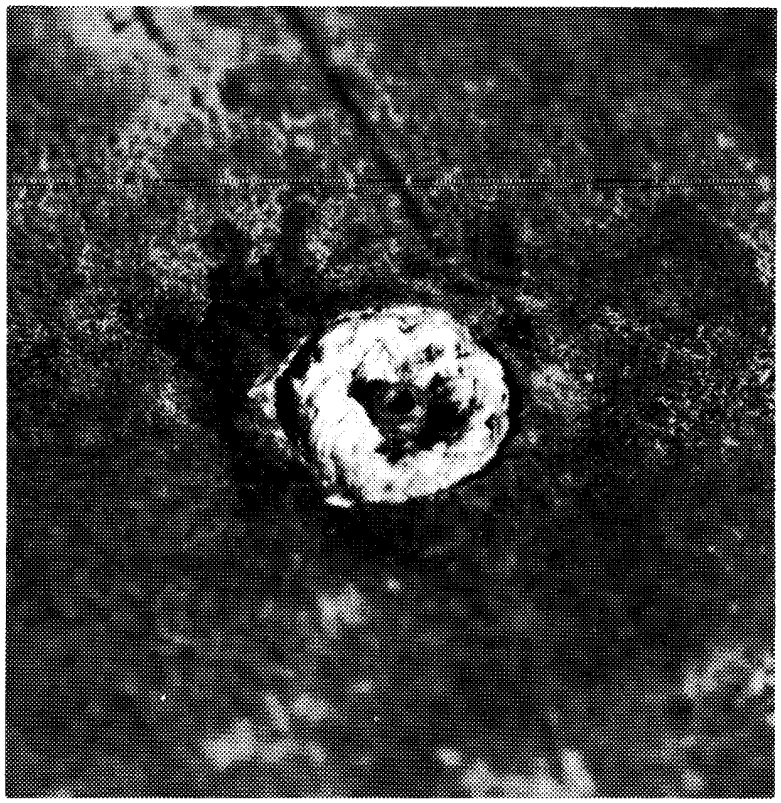

Figure 2. Postflight condition of typical STS 61-C TPS tile orifice.

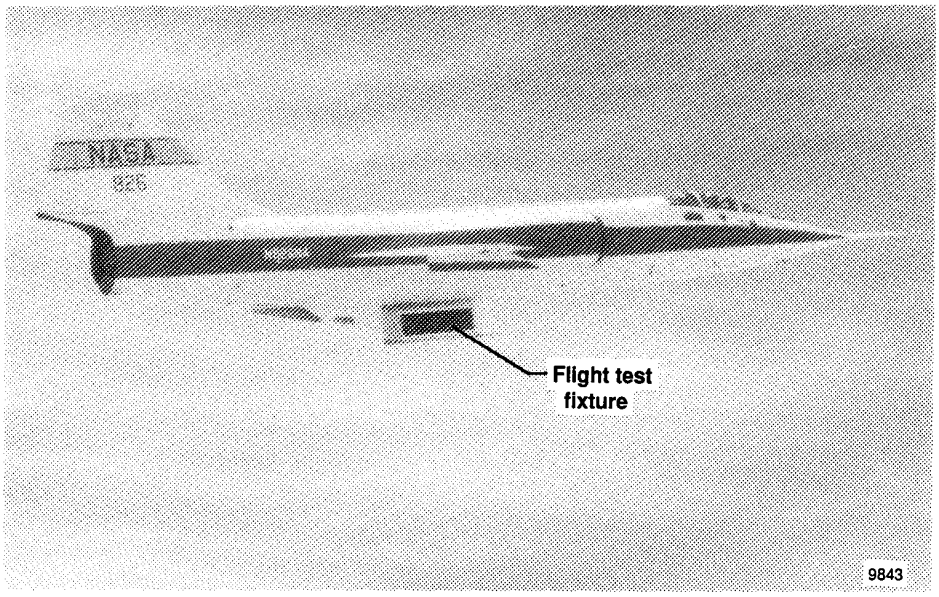

(a). Aircraft with the FTF mounted beneath the fuselage.

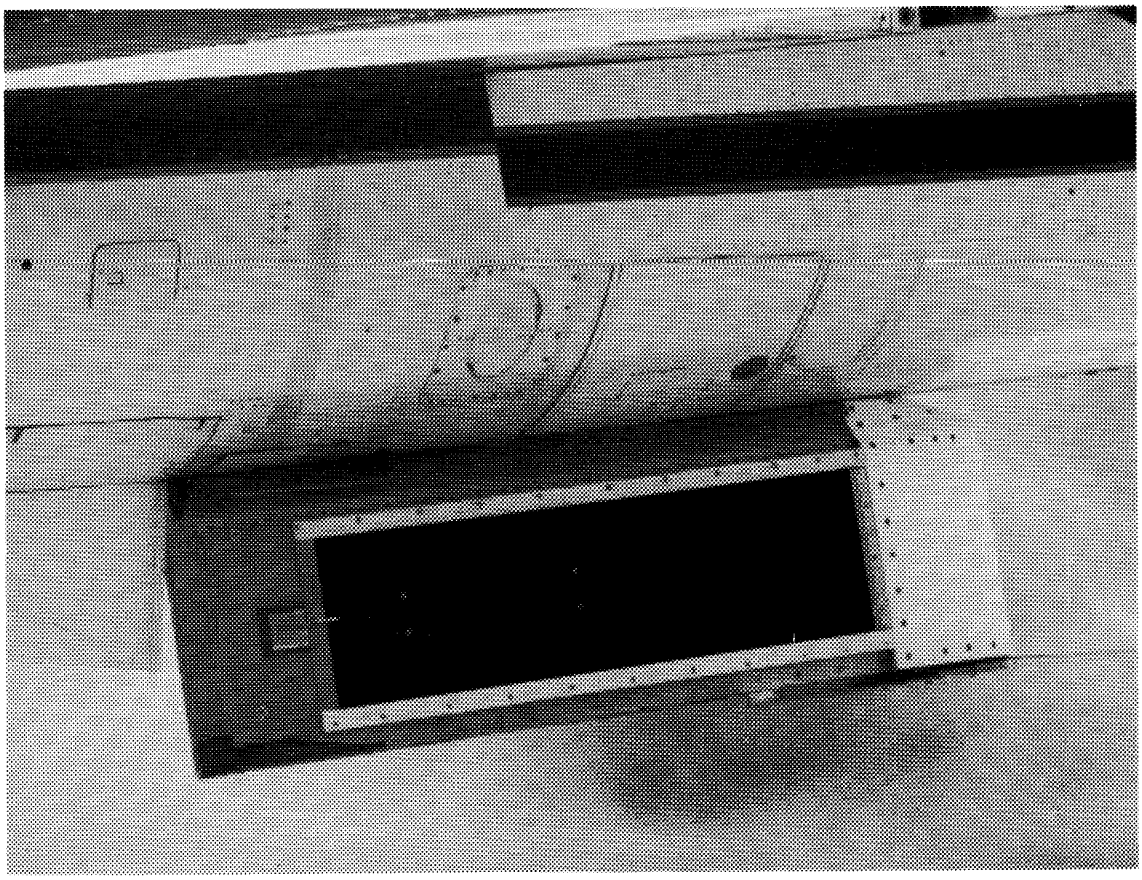

(b) The FTF with test panel installed.

Figure 3. The F-104 aircraft in flight.

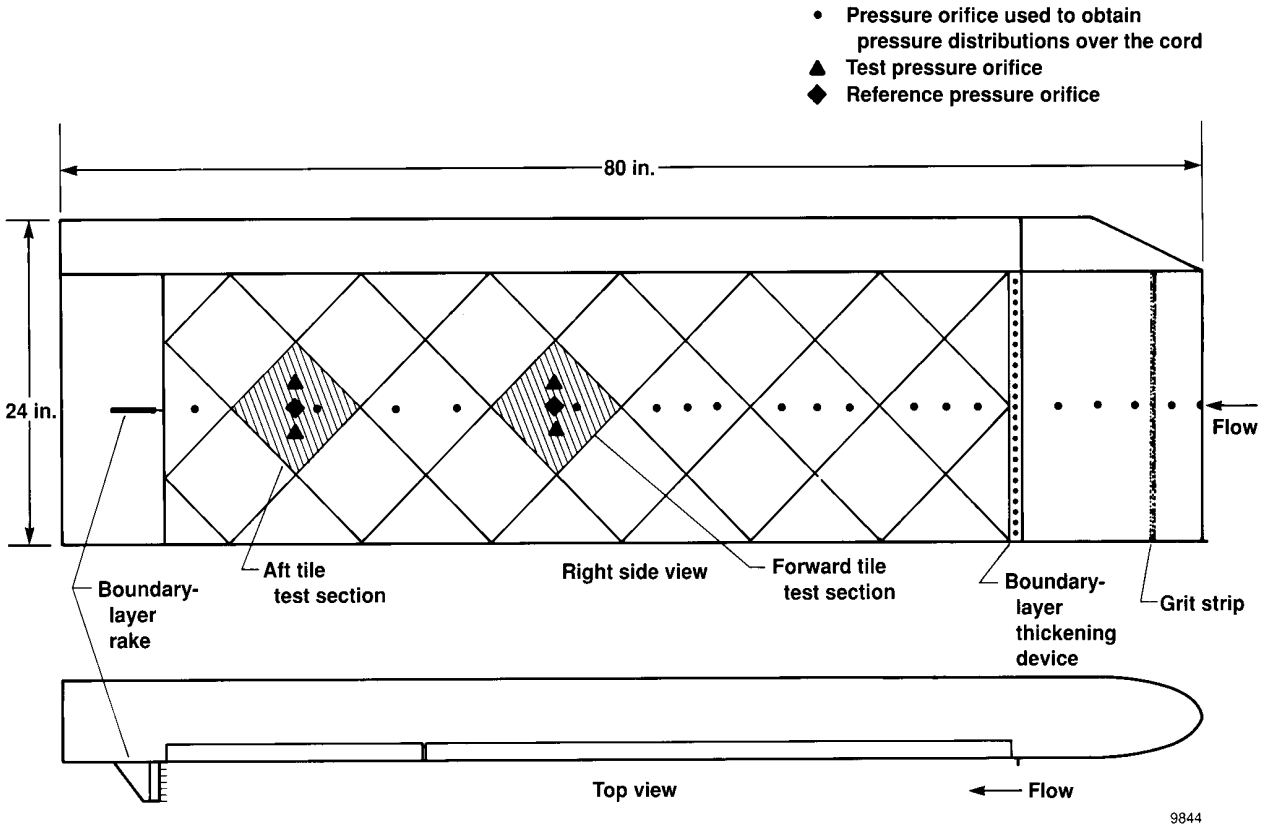

Figure 4. The FTF with tile test articles locations.

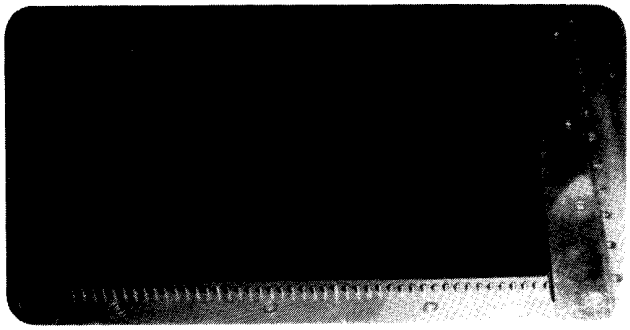

Installed on aircraft

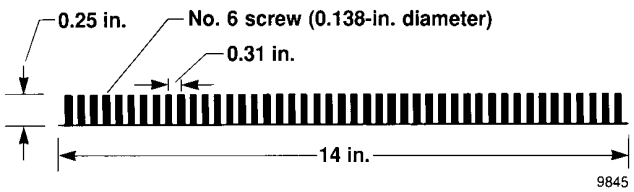

Figure 5. Boundary-layer thickening device.

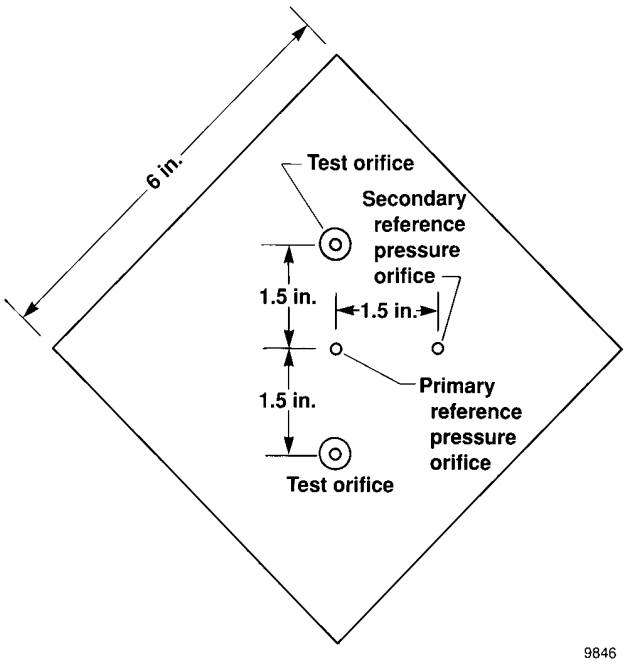

(a) Planform.

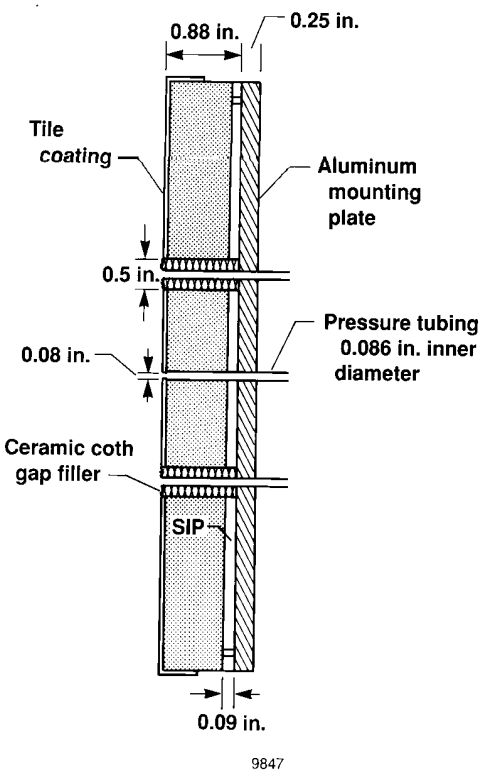

(b) Tile cross section with SIP.

Figure 6. Test article configuration.

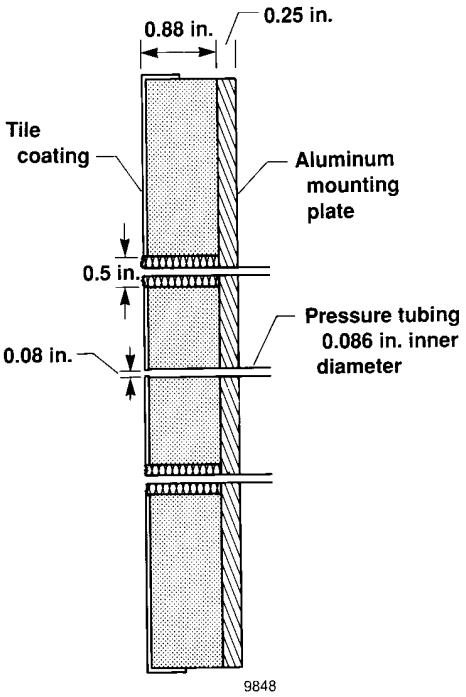

(c) Tile cross section without SIP.

Figure 6. Concluded.

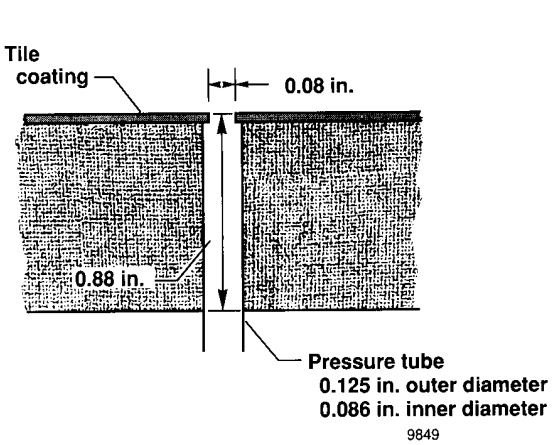

(a) Reference orifices R1 to R4.

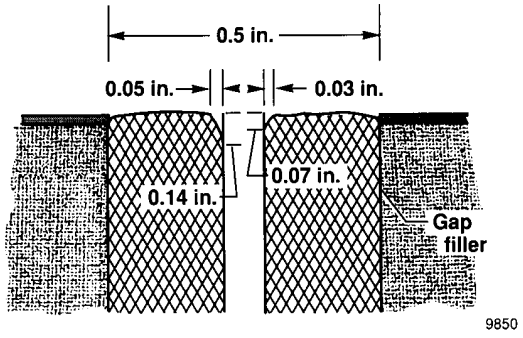

(b) Orifice 1.

Figure 7. Orifice installations.

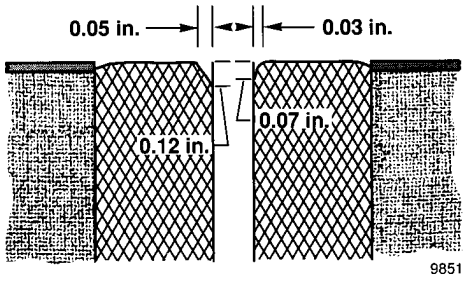

(c) Orifice 2.

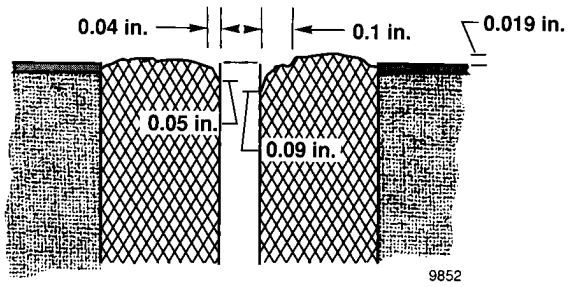

(d) Orifice 3.

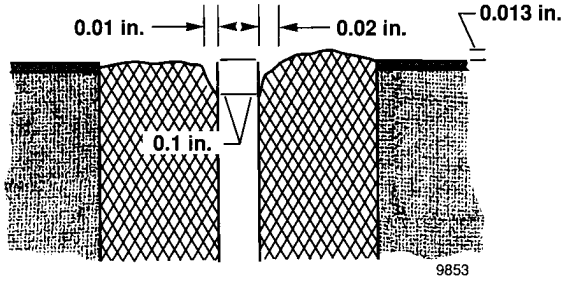

(e) Orifice 4.

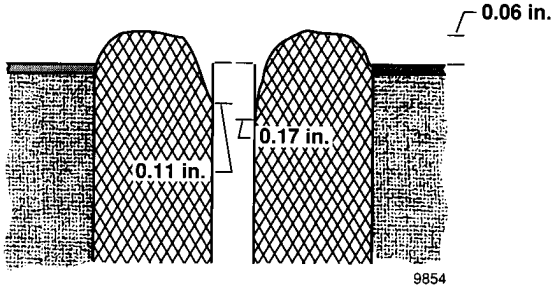

(f) Orifice 5.

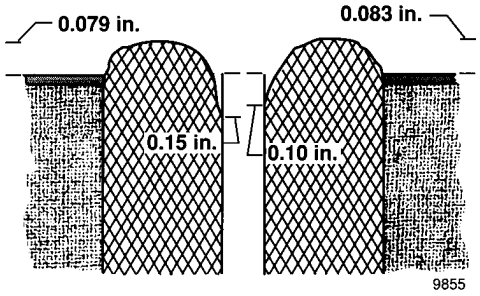

(g) Orifice 6.

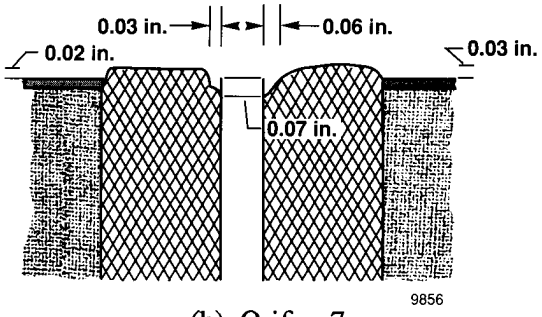

(h) Orifice 7.

Figure 7. Continued.

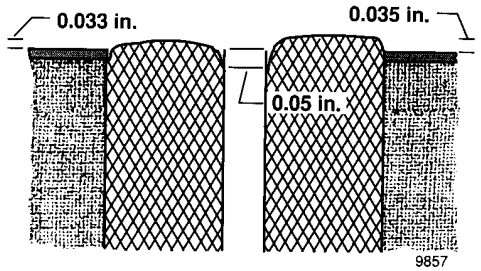

(i) Orifice 8.

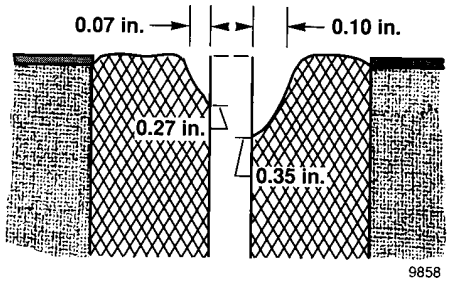

(j) Orifice 9.

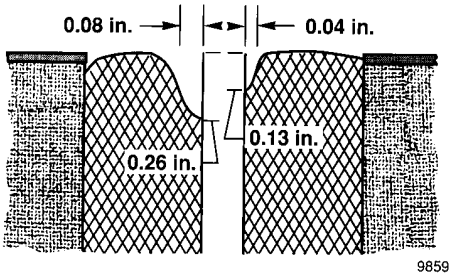

(k) Orifice 10.

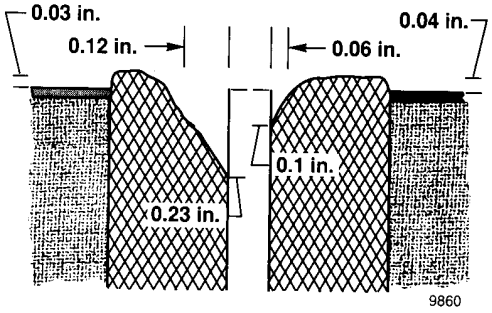

(l) Orifice 11.

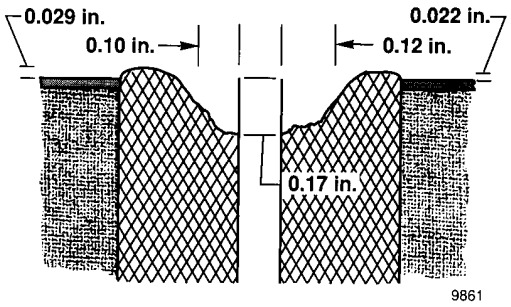

(m) Orifice 12.

Figure 7. Concluded.

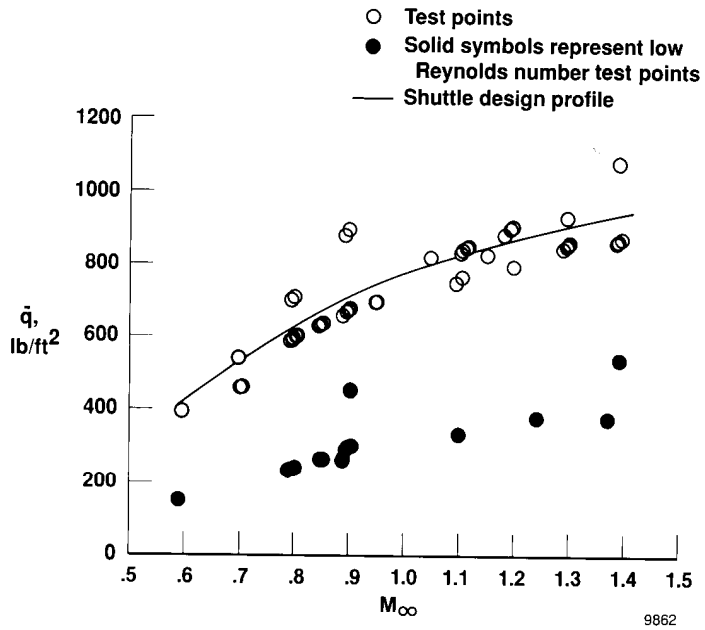

Figure 8. Dynamic pressure and Mach numbers for test conditions.

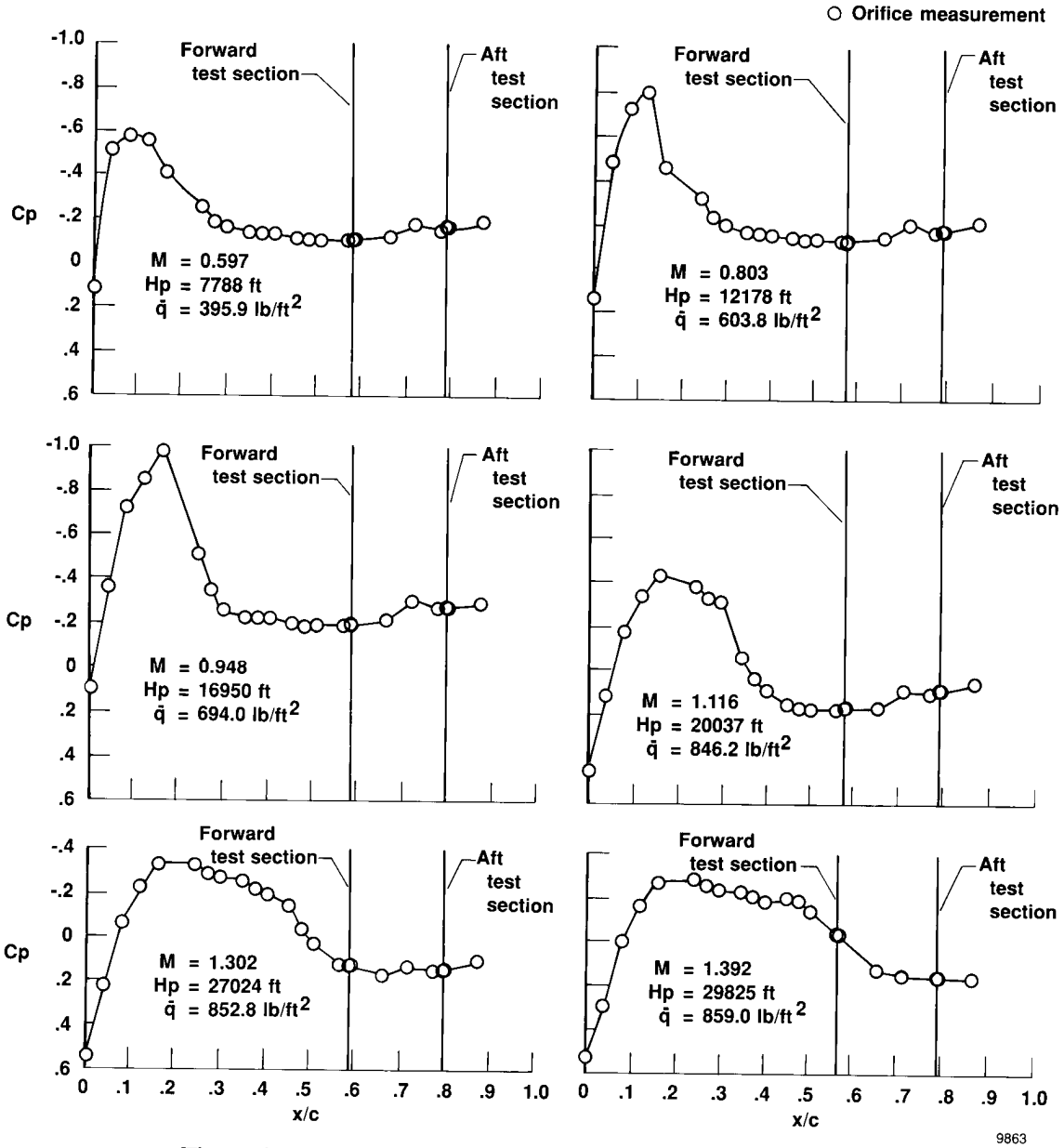

Figure 9. Typical FTF pressure distributions along the chord.

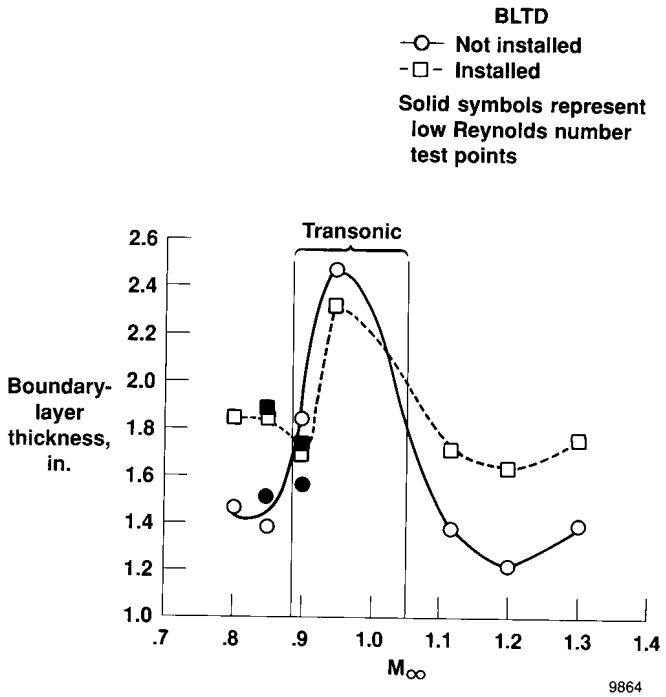

Figure 10. The effects on FTF boundary-layer thickness of the BLTD and of decreased Reynolds number.

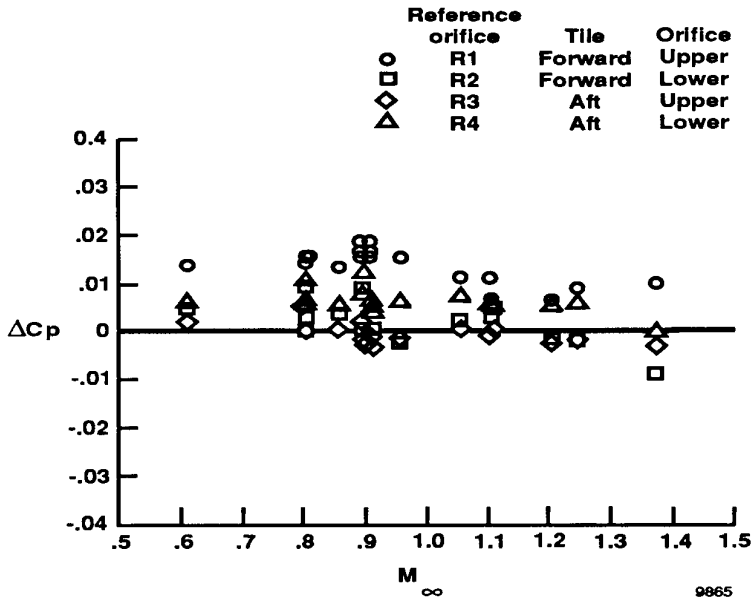

(a) The ΔCp.

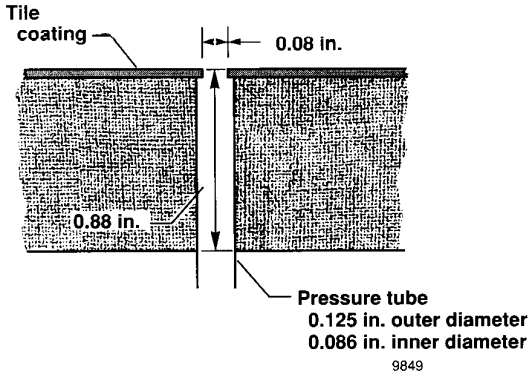

(b) Reference orifices R1 to R4.

Figure 11. Reference orifices R1 to R4 without the BLTD.

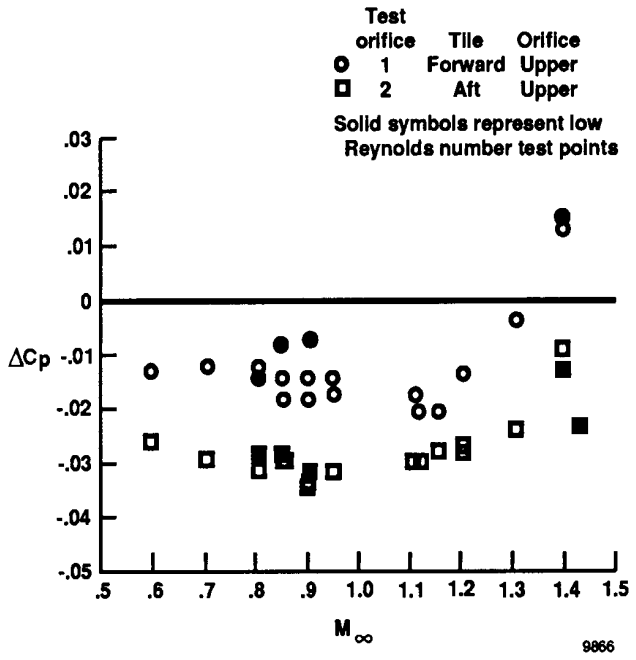

(a) The ΔCp with the BLTD.

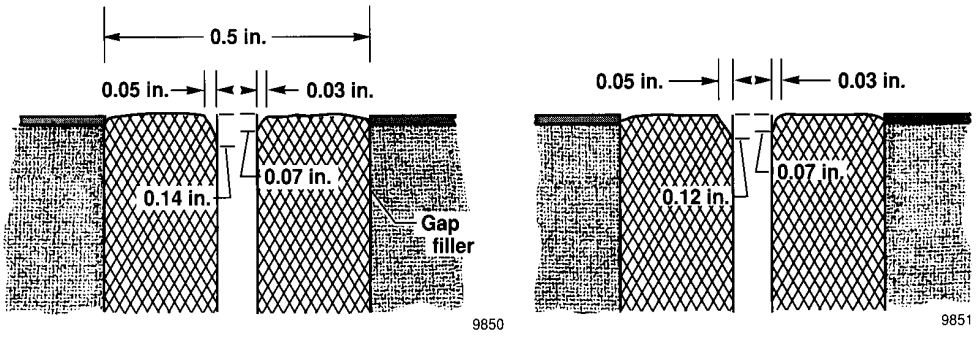

(b) Test orifices 1 and 2.

Figure 12. Measurements for test orifices 1 and 2.

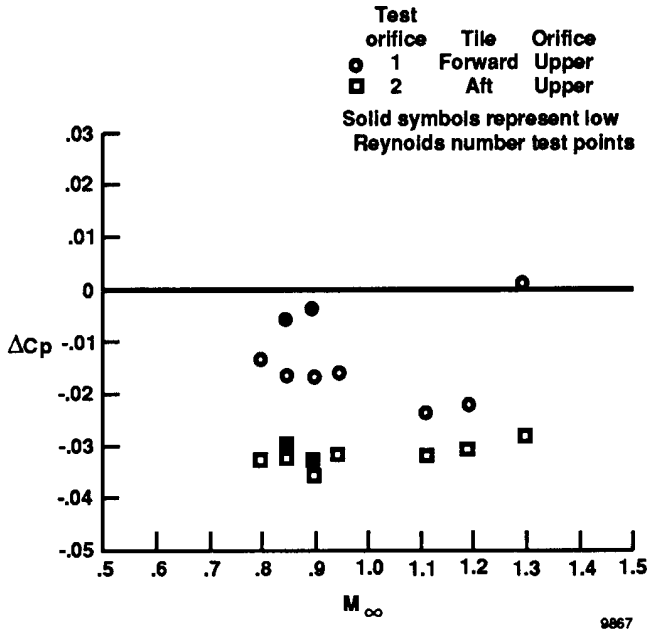

(c) The ΔCp without the BLTD.

Figure 12. Concluded.

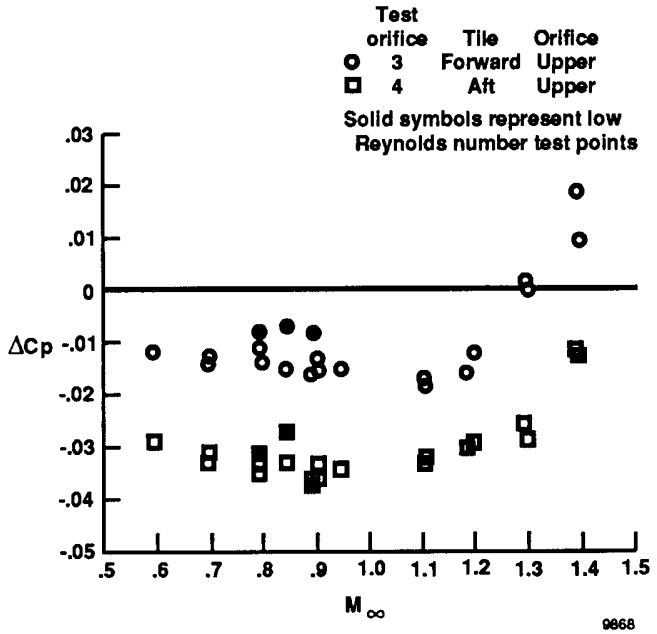

(a) The ΔCp with the BLTD.

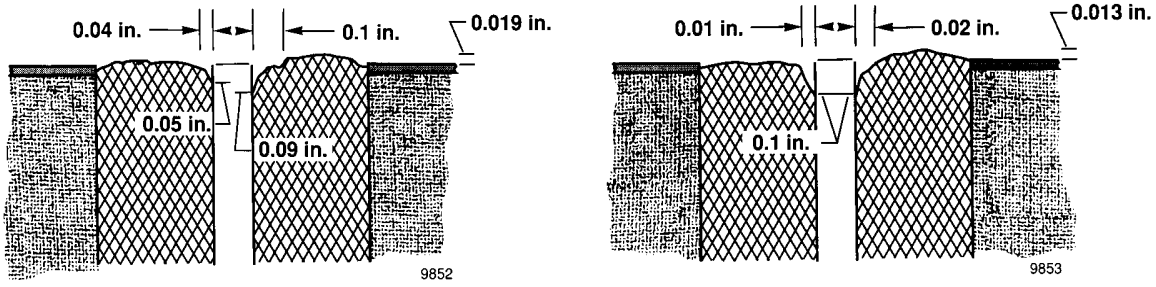

(b) Test orifices 3 and 4.

Figure 13. Measurements for test orifices 3 and 4.

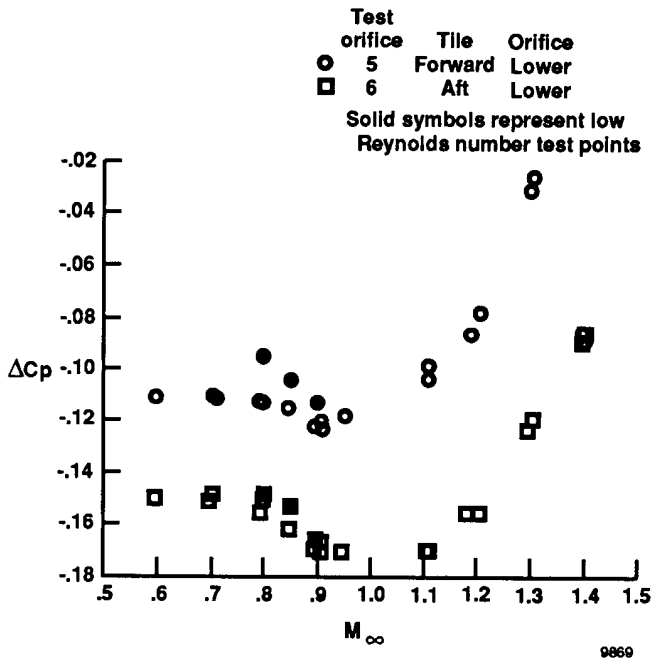

(a) The ΔCp without the BLF.

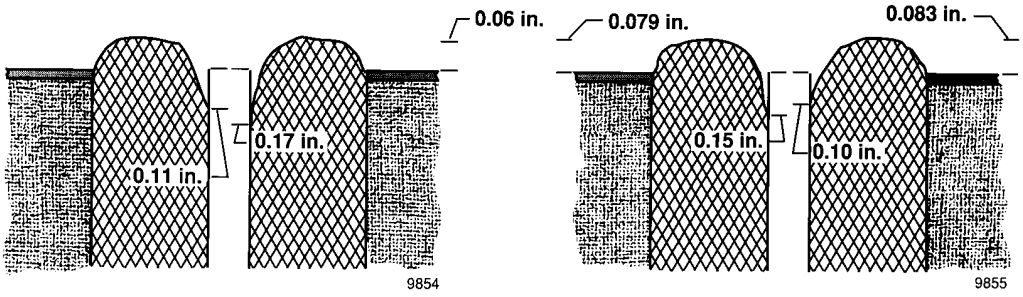

(b) Test orifices 5 and 6.

Figure 14. Measurements for test orifices 5 and 6.

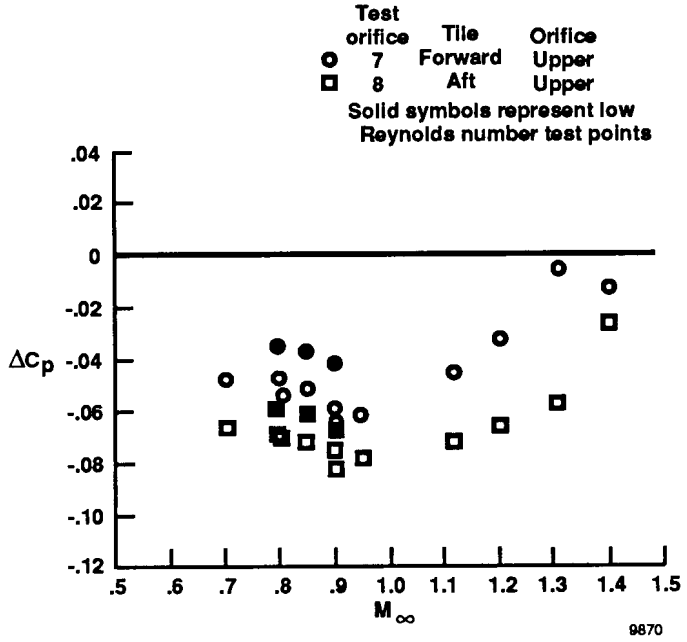

(a) The ΔCp with the BLTD.

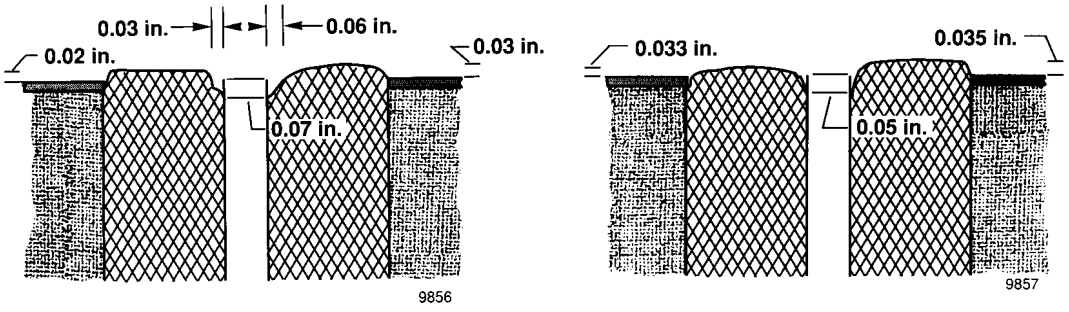

(b) Test orifices 7 and 8.

Figure 15. Measurements for test orifices 7 and 8.

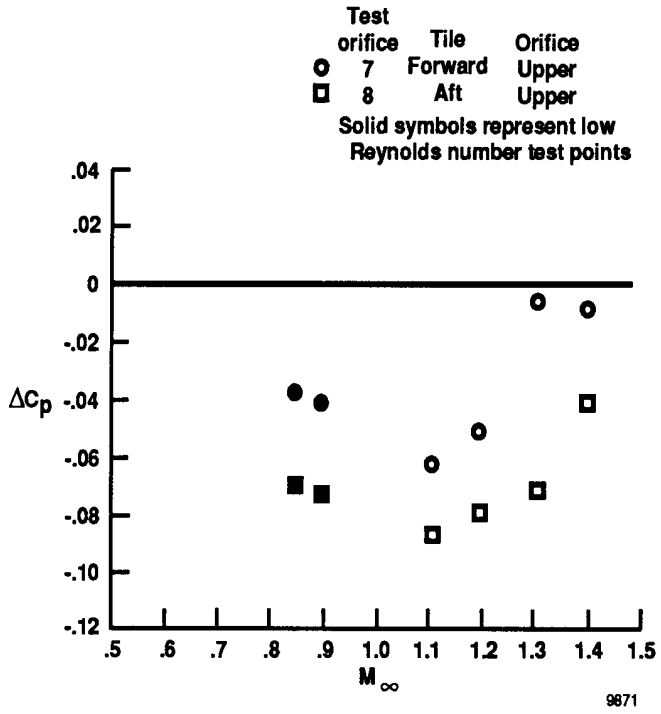

(c) The ΔCp without the BLTD.

Figure 15. Concluded.

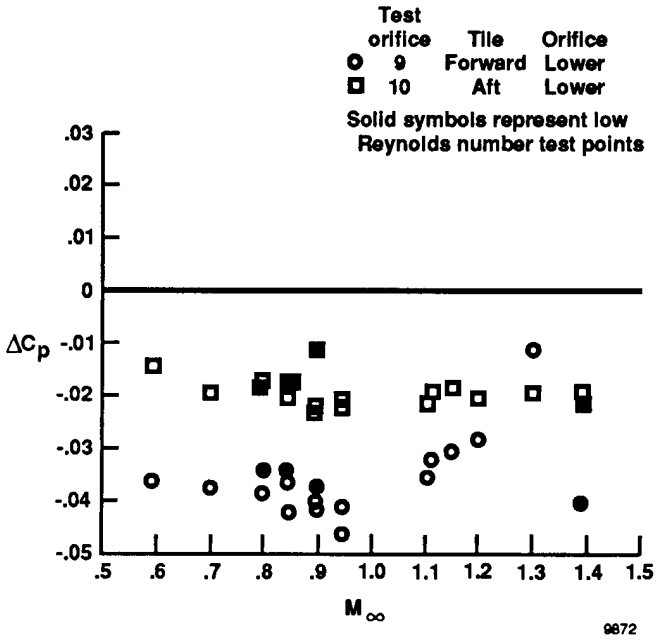

(a) The ΔCp with the BLTD.

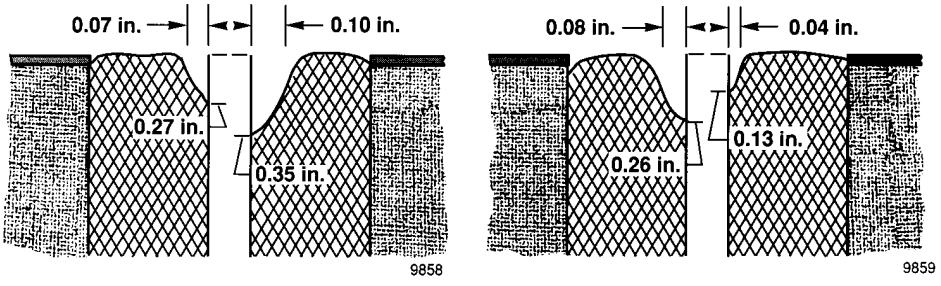

(b) Test orifices 9 and 10.

Figure 16. Measurements for test orifices 9 and 10.

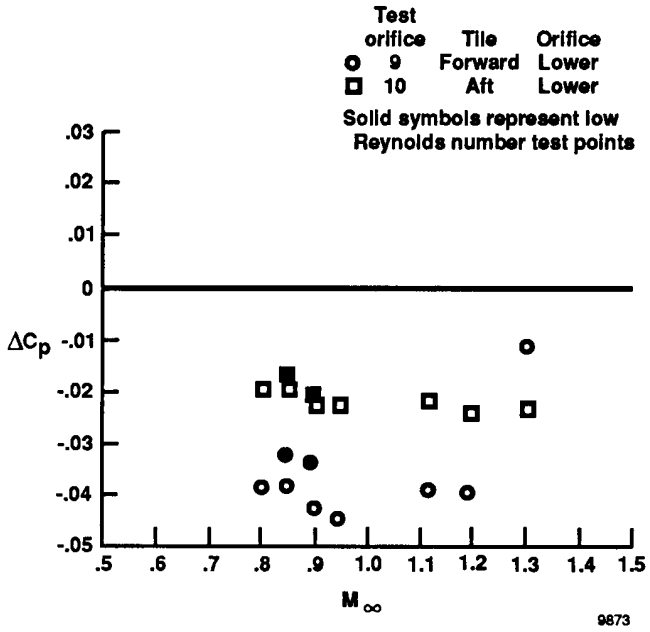

(c) The ΔCp without the BLTD.

Figure 16. Concluded.

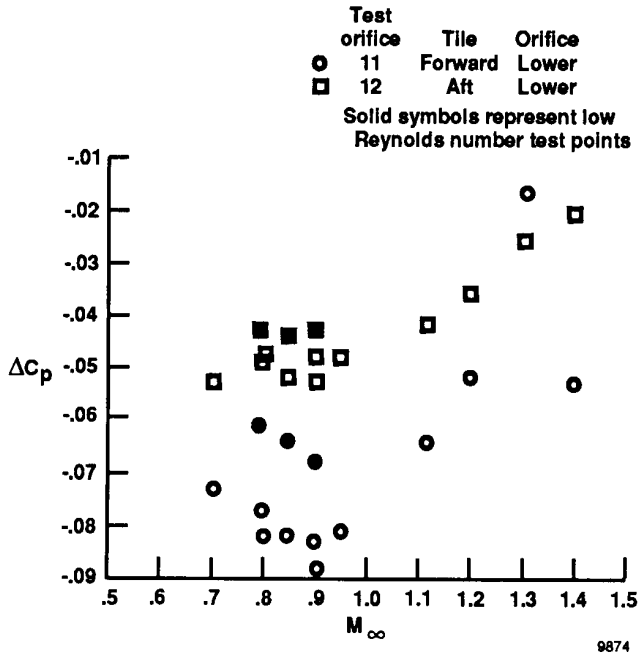

(a) The ΔCp with the BLTD.

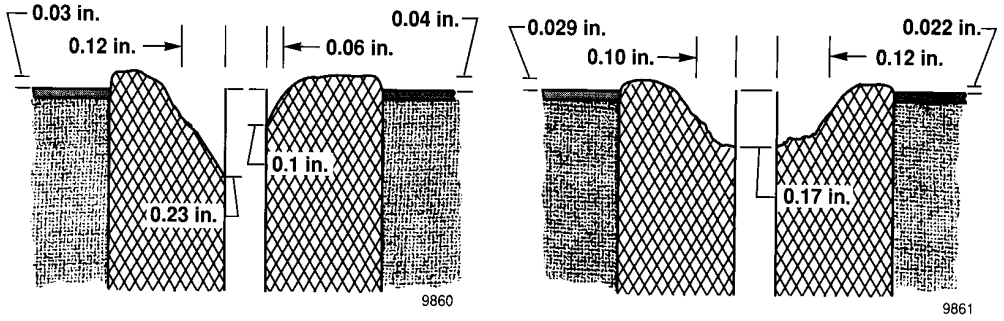

(b) Test orifices 11 and 12.

Figure 17. Measurements for test orifices 11 and 12.

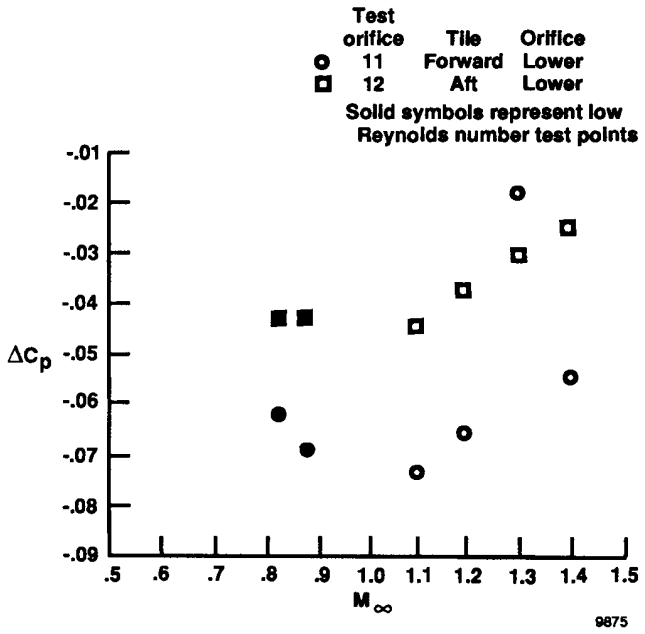

(c) The ΔCp without the BLTD.

Figure 17. Concluded.

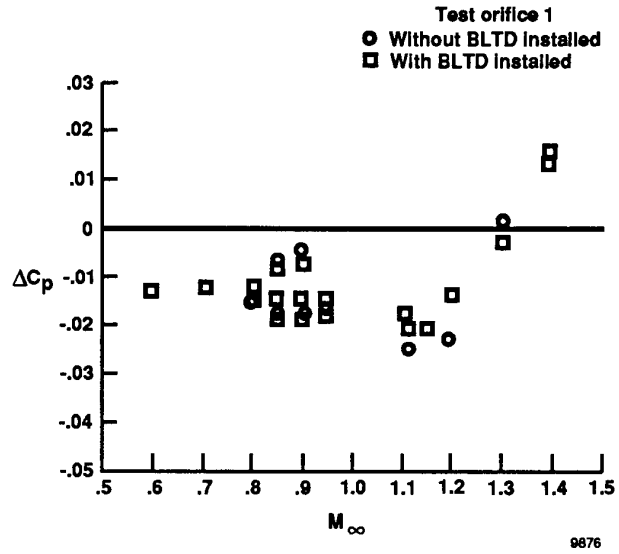

(a) Test orifice 1.

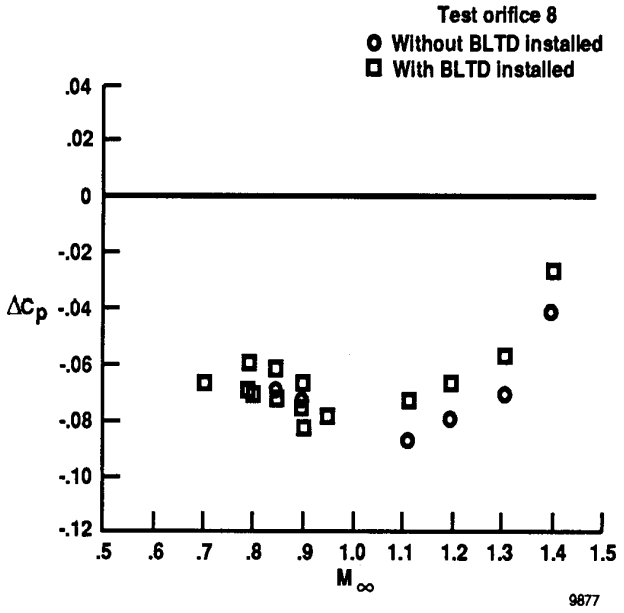

(b) Test orifice 8.

Figure 18. Affects of the BLTD on ΔCp.

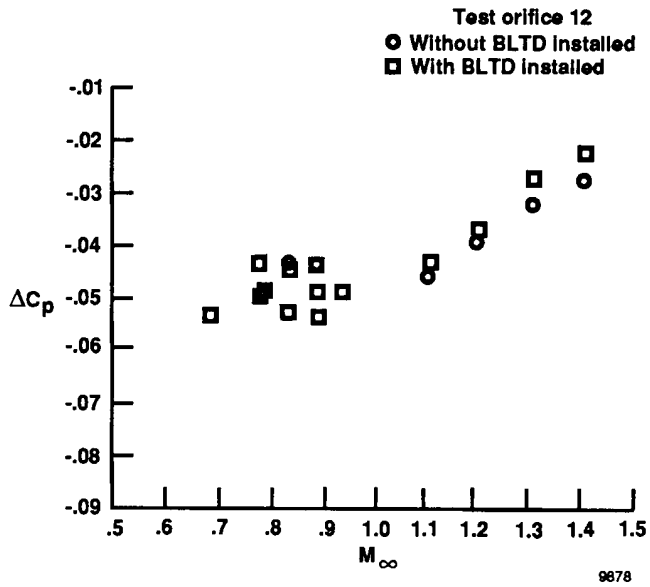

(c) Test orifice 12.

Figure 18. Concluded.

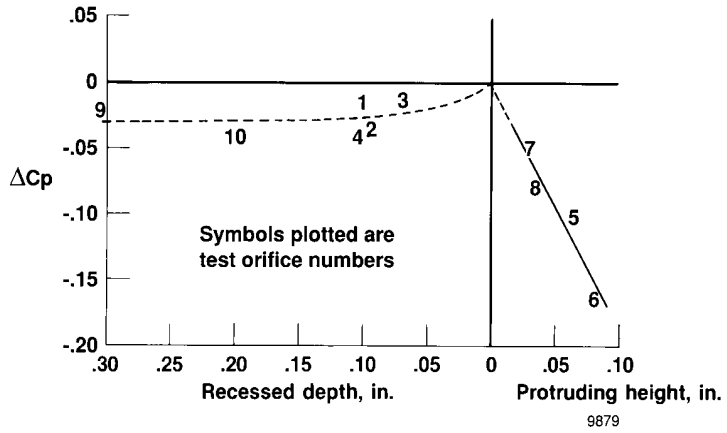

Figure 19. Affect of surface anomalies on orifice measurement errors.

NASA
National Aeronautics and Space Administration

Report Documentation Page

1. Report No.	2. Government Accession No.	3. Recipient's Catalog No.
NASA TM-4219		

4. Title and Subtitle	5. Report Date
In-Flight Investigation of Shuttle Tile Pressure Orifice Installations	September 1990
	6. Performing Organization Code

7. Author(s)	8. Performing Organization Report No.
Timothy R. Moes and Robert R. Meyer, Jr.	H-1575
	10. Work Unit No. RTOP 505-61-41

9. Performing Organization Name and Address	11. Contract or Grant No.
NASA Ames Research Center Dryden Flight Research Facility P.O. Box 273, Edwards, California 93523-0273	
	13. Type of Report and Period Covered Technical Memorandum
12. Sponsoring Agency Name and Address National Aeronautics and Space Administration Washington, DC 20546-3191	14. Sponsoring Agency Code

15. Supplementary Notes

16. Abstract

To determine shuttle orbiter wing loads during ascent, wing load instrumentation was added to Columbia (0V-102). This instrumentation included strain gages and pressure orifices on the wing. The loads derived from wing pressure measurements taken during STS 61-C did not agree with those derived from strain gage measurements or with the loads predicted from the aerodynamic database. Anomalies in the surface immediately surrounding the pressure orifices in the thermal protection system (TPS) tiles were one possible cause of errors in the loads derived from wing pressure measurements. These surface anomalies were caused by a ceramic filler material which was installed around the pressure tubing. The filler material allowed slight movement of the TPS tile and pressure tube as the airframe flexed and bent under aerodynamic loads during ascent and descent. Postflight inspection revealed that this filler material had protruded from or receeded beneath the surface, causing the orifice to lose its flushness. Flight tests were conducted at the National Aeronautics and Space Administration (NASA) Ames Research Center Dryden Flight Research Facility to determine the effects of any anomaly in surface flushness of the orifice installation on the measured pressures at Mach numbers between 0.6 and 1.4. An F-104 aircraft with a flight test fixture mounted beneath the fuselage was used for these flights. Surface flushness anomalies typical of those on the orbiter after flight {STS 61-C} were tested. Also, cases with excessive protrusion and recession of the filler material were tested.

This report shows that the anomalies in STS 61-C orifice installations adversely affected the pressure measurements. But the magnitude of the affect was not great enough to account for the discrepancies with the strain gage measurements and the aerodynamic predictions.

17. Key Words (Suggested by Author(s))	18. Distribution Statement
Pressure Orifices Pressure measurement errors Shuttle tile	Unclassified-Unlimited Subject Category 34

19. Security Classif. (of this report)	20. Security Classif. (of this page)	21. No. of Pages	22. Price
Unclassified	Unclassified	36	A03

NASA FORM 1626 OCT 86 *For sale by the National Technical Information Service, Springfield, Virginia 22161-2171*

NASA-Langley, 1990